ELECTROCHEMICAL MODELING AND FRACTURE MECHANICS TESTING TO MITIGATE ENVIRONMENTALLY ASSISTED CRACKING OF MULTI-MATERIAL ASSEMBLIES

Victor Kontopanos, Daniel Stokes, & Dr. Robert Kelly
Department of Materials Science and Engineering, University of Virginia

Abstract

Finite element method modeling used in conjunction with electrochemical kinetics is a powerful tool for understanding observable phenomena. Multi-component, multi-material assemblies often exhibit corrosion and cracking problems that occur from atmospheric electrolytes. This work focuses on mitigating galvanically induced environment assisted cracking on Pyrowear 675 steel from anodized titanium through the application of an anodic ZnNi plating. From crack growth rates published in literature, a target potential for the material down the fastener hole of the multi-component assembly was acquired. The P675 substrate was found to have a wide range of variability in the measured electrochemical kinetics, leading to some instances that would cause cracking to be expected and other instances when it would not be for the same geometry and wetting conditions in 0.6M NaCl. The as-manufactured ZnNi plating is highly active and too polarizing, pulling the P675 down below the immunity well (< -700mV$_{SCE}$). The ZnNi underwent self-ennoblement at OCP with the measured potential increasing slowly. FEM simulations conducted for partial wetting on the surface and down the fastener hole indicated there is a risk of cracking for P675 with initial and 3-week ZnNi kinetics, but that the risk is removed for exposures of 6 weeks and beyond.

Introduction

Aerospace structures often use multi-material systems to satisfy the engineering requirements for their strenuous applications. High strength steels such as Pyrowear 675 are widely used as structural alloys in aerospace applications.[1–3] These types of materials have been known to experience environmentally assisted cracking (EAC) problems due to accelerated crack growth rate from hydrogen that is produced as a corrosion product.[2–5] High residual stresses around fasteners along with galvanic coupling from dissimilar materials can lead to the accumulation of aggressive corrosive species, acidified solution, pitting damage, and potentially crack propagation.[6,7] The crack growth rate has been shown to be dependent on potential for certain classes of materials, which includes P675.[1–3,8] Recently published literature has showcased work that indicates a region of low crack growth rate for P675 in 0.6M NaCl environments, Figure 1.[1,2]

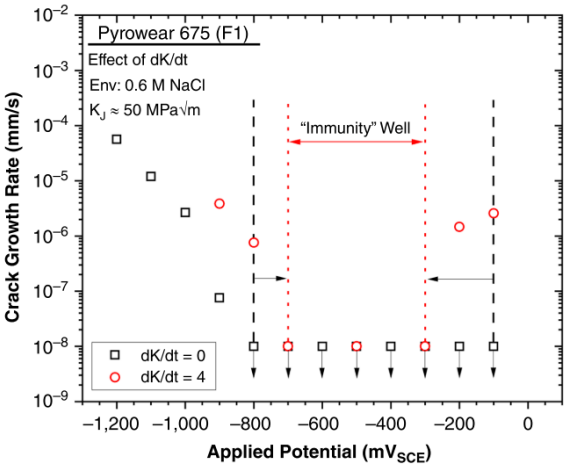

Figure 1. *Affect of the applied potential on the crack growth rate of P675 immersed in 0.6M NaCl under two different loading rates (dK/dt = 0 and 4). Note that use of 10^{-8} mm/s for the lack of EAC susceptibility is arbitrary and does not have any quantitative significance.*[2]

Marshall et al. showed that the ability of the anodized Ti fastener to polarize the P675 up to higher potentials, outside the low cracking regime from -300 to -700 mV$_{SCE}$, which leads to an increased risk of cracks propagating.

One possible solution to this cracking problem is to use a sacrificial ZnNi plating applied to the P675 to counteract the polarization of anodized Ti.[1,2] Using ZnNi plating as another material in the system could allow for the control of the potential down the fastener hole to be within the window of low crack growth rate. The work outlined in this paper has been conducted to evaluate the option to apply this ZnNi plating to P675 to resolve cracking problems that have been observed in engineering applications.

The objective of this work to devise a solution to mitigate the risk for EAC on P675 when coupled to anodized Ti through the use of a ZnNi plating leveraged a combination of electrochemical testing and finite element method modeling.

Experimental Procedures

Materials

All of the materials tested were provided by Rolls-Royce Corporation and or Techmetals Inc. The Pyrowear 675 used for electrochemical measurements was all sourced from components. Anodized titanium bolts were provided for electrochemical measurements. ZnNi samples were provided from different batches on different substrates. Many ZnNi samples were plated using the standard bath and process from Techmetals Inc. both on P675 and carbon steel substrates.

Boundary Condition Generation

The potentiodynamic polarization scans (PDS) were performed with samples set up in full immersion conditions using a conventional three electrode flat cell with Ag/AgCl as the reference. The potentials were converted to SCE using a potential offset based on measurements of the reference electrode(s) vs an SCE mother electrode at the Center for Electrochemical Science and Engineering at the University of Virginia. A Pt mesh was used as the counter electrode for all tests. A scan rate of 10mV/s was used based on previous work.[2] The measured current was converted to current density by normalizing with the exposed surface area, generally either 0.1 cm^2 or 1 cm^2 depending on the sample.

Anodic polarization curves were collected on as received ZnNi samples and P675 samples in an as received state and polished to 400 grit with SiC. A 0.6M NaCl was used for all anodic tests. These PDS were collected following a 30 min OCP exposure by scanning in the electropositive direction up to -550 mV_{SCE} starting 20 mV below the measured OCP.

Cathodic polarization curves were collected on as received P675 samples and those polished to 400 grit with SiC in 0.6M Na_2SO_4. These PDS were collected following a 30 min OCP exposure by scanning in the electronegative direction down to -1.5 V_{SCE} starting 20 mV above the measured OCP. Similar tests were conducted on the anodized Ti.

Galvanic Couple Exposures

The galvanic coupling exposures were set up in a conventional flat cell set up with one sample on either end. A three-electrode set up was used with Ag/AgCl as the reference electrode and the cathodic material as the counter electrode and anodic material as the working electrode. Exposures were conducted in 0.6M NaCl.

Galvanostatic Zn dissolution exposures

Each test was set up in a flat cell with a standard three electrode set up. Prior to galvanostatic exposure, a 30 min OCP was conducted to ascertain the initial potential of the ZnNi plating. The galvanostatic exposure followed either a single continuous exposure at the specified current for the desired duration or a cyclic test. For a cyclic test, following the initial OCP measurement, a sample would undergo a galvanostatic exposure followed by another OCP measurement to gauge the degree of ennoblement, Figure 2.

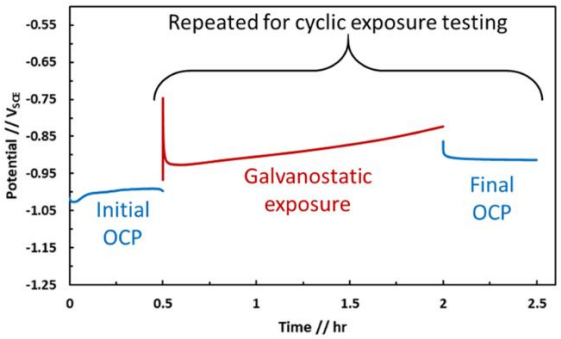

Figure 2. *Galvanostatic exposure procedure.*

These alternating galvanostatic exposures and OCP measurements were continued until the total time of dissolution had been reached. After each galvanostatic treatment was fully concluded, either for cyclic or continuous, a final 30 min OCP was collected to determine the final potential.

Finite Element Method Modeling

All models were built and run using version 6.1 of the COMSOL Multiphysics© FEM modelling software with a secondary current distribution from the corrosion module. Several

geometries were constructed with the incorporation of experimentally determined boundary conditions to act at the kinetic behavior of the different solution metal interfaces from the multi-material assembly. Several important assumptions were made:

1. Steady state conditions over the system to allow for the use of the Laplace equation in the simulations.
2. A conformal electrolyte water layer over the assembly and down through the gaps.
3. The dominating means of mass transport was assumed to be migration. Diffusion and convection were ignored.

One main model was constructed in this work to closely capture the geometric complexities of the multi-component assembly: noble fastener set to hold multiple plates together, Figure 3.

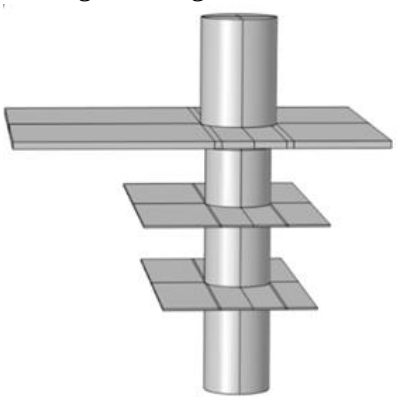

Figure 3. *3D rendering of the conformal WL over the multi-component assembly.*

The gaps in the assembly were built to match those from the design for the multi-component assembly provided by Rolls-Royce. The overall WL of the main model underwent modifications to account for different possible wetting scenarios. The impact of ZnNi plating location, boundary condition variations, and partial wetting conditions were studied in this work.

Results

Potentiodynamic & Galvanic Polarizations

Individual polarization experiments were performed to ascertain the electrochemical behavior of the P675, ZnNi plating, and anodized Ti that was necessary for FEM modeling boundary conditions, Figure 4.

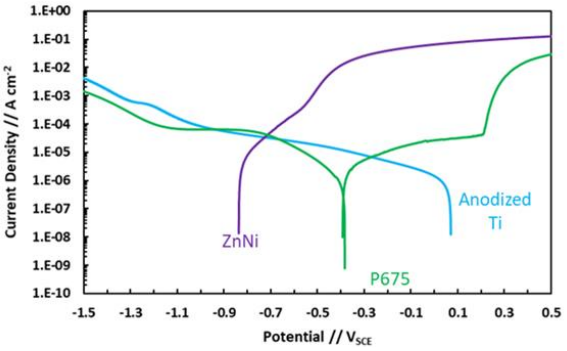

Figure 4. *Representative PDS curves acquired on ZnNi (anodic), P675 (anodic and cathodic run separately), and anodized Ti (cathodic) in 0.6M NaCl following 30 min OCP, dE/dt = 10 mV s^{-1}, 25C.*

The polarization curves for the different batches of ZnNi plating indicate high variability, potentially due to microstructure or chemical heterogeneity. The OCPs and kinetics observed from the PDS in Figures 5 for the ZnNi plating in an as manufactured condition are too anodic in nature to be viable for use in service to counteract the effect of the polarization of the anodized Ti on the P675.

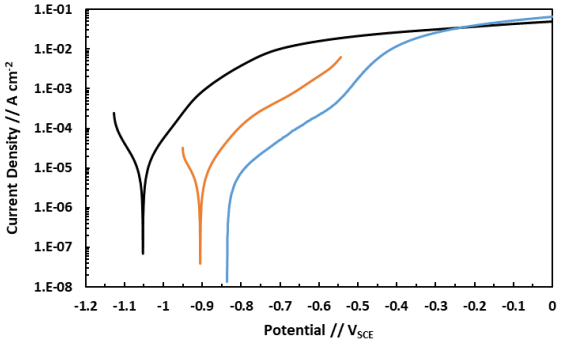

Figure 5. PDS acquired on ZnNi plating on different batches and sample substrates from Techmetals Inc following 30 min OCP, 0.6M NaCl solution, dE/dt = 10 mV s^{-1}, 25C.

There is a large range in OCP measured across these different batches, upwards of 200 mV. These ZnNi platings will lead to overpolarization, which in turn puts the P675 at a potential of high cracking below the immunity well. In order to illustrate this, a galvanic exposure test was conducted with each individual material being measured separately prior to the coupling. Figure 6 shows the OCP plots for P675 and ZnNi prior to coupling and then what

happens to the potential measured when they are galvanically coupled in the same solution.

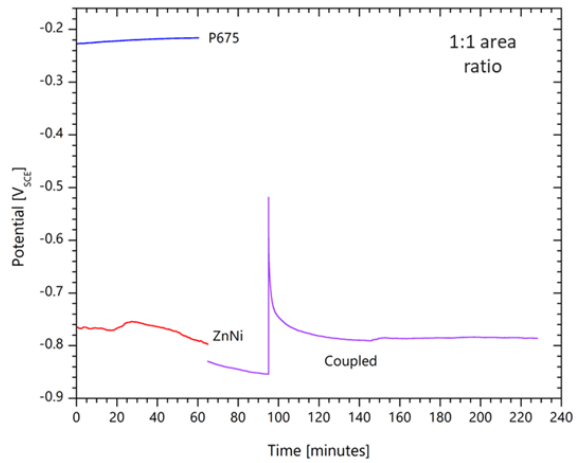

Figure 6. *OCP measured for ZnNi and P675 individually and then the potential once the two materials are coupled together in 0.6M NaCl, 25C.*

The sequential potential measurements of ZnNi and P675 individually and then coupled clearly show the polarizing capability of ZnNi. For the 1:1 area ratio used, the ZnNi pulls the P675 all the way down to the ZnNi OCP value.

The polarizing capability of the ZnNi necessitated an investigation into changing the kinetics in an effort to have a plating that will not lead to over polarization and exacerbated cracking. If variation in the chemical composition can be controlled, then it may be possible to have a ZnNi plating with a target OCP desired. An evolving OCP with a wide range of bounds was observed in long exposures, up to ten weeks, of ZnNi conducted in 0.6M NaCl. The evolution of measured OCP versus time can be seen in Figure 7a while the changes observed in the kinetics (PDS curves) are shown in Figure 7b.

The rise of potential observed of ZnNi during open circuit exposure shows that there is a self-ennoblement process such that its OCP will eventually reach the low cracking regime. This self-ennoblement is further corroborated with the PDS gathered along the way in this long-term exposure. After weeks of exposure, the over polarization and cracking risk from ZnNi would be expected to decrease due to the ennoblement of the plating to higher OCP with increasing exposure time.

SEM-EDS analysis of the ZnNi at several stages throughout a long OCP exposure indicate that enrichment of Ni from the starting composition (15.8wt.%) up to nearly 25 wt.% can be achieved. This enrichment of Ni observed corroborated the theory that the ennoblement is due to the dissolution of Zn from the matrix. A ZnNi plating with composition of the surface after six or more weeks would be a good option to use in service if it can be manufactured with that chemistry; this would prevent the risk of over polarizing the P675.

An effort was made to speed up the self-ennoblement process observed for the ZnNi plating under OCP conditions and develop a post-processing method to enrich the Ni content of the plating through using a galvanostatic (i.e., constant applied current) exposure technique.

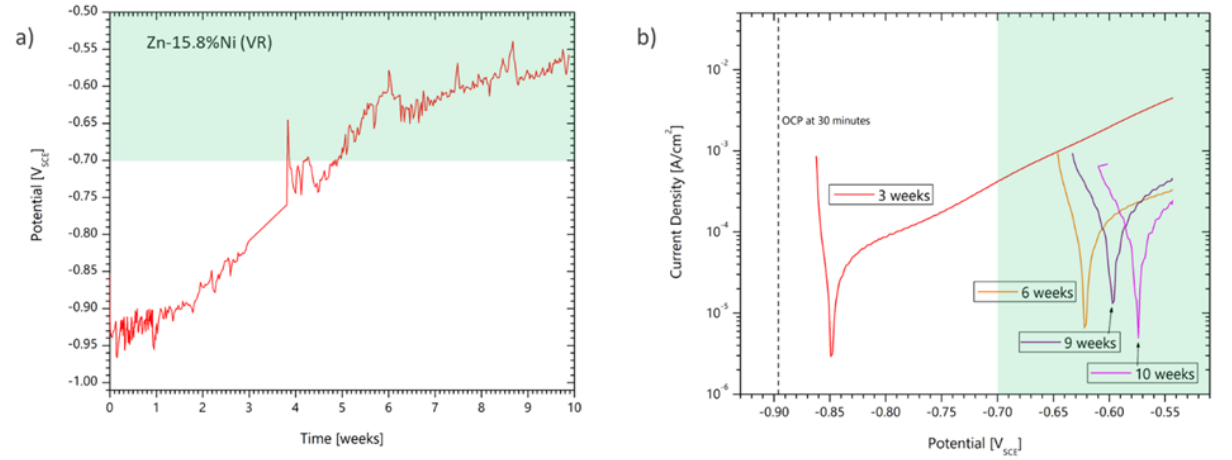

Figure 7. *(a) OCP of ZnNi plated on P675 measured in 0.6M NaCl for ten weeks (b) series of PDS curves generated on ZnNi surfaces from 3 up to 10 weeks.*

Galvanostatic exposures

In this procedure, an initial OCP is was measured before any dissolution occurred with the applied current of the galvanostatic exposure. Following that OCP measurement, the sample is subjected to a galvanostatic exposure and then an OCP measurement after dissolution. There are many possible parameters that can affect the ennoblement process including the initial OCP of the ZnNi plating, the time of galvanostatic exposure, the current applied, whether the exposure is continuous or cyclic, and the solution in which the dissolution takes place.

The blue curve in Figure 8 is representative of a continuous exposure with an initial and final OCP measured on either end of the treatment. The black curves are from a cyclic exposure that alternated between 30 min OCPs and 90 min galvanostatic dissolution exposures with a total dissolution time of twelve hours. Each test also had a two-hour OCP after to examine the stability of this value. The cyclic exposure was able to reach a higher potential through ennoblement and had a more stable OCP after this treatment.

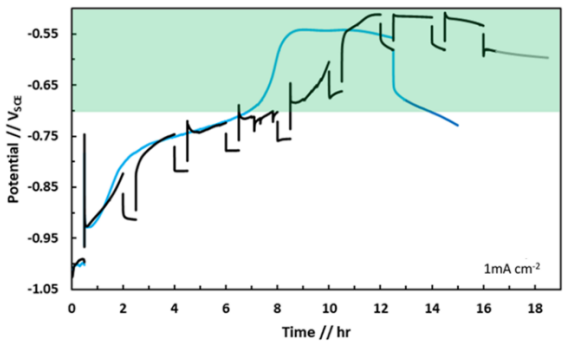

Figure 8. *Measured potential during forced Zn dissolution procedure of OCP, 1mA cm^{-2} galvanostatic exposure either continuous or cyclic for a total time of 12hr, and 2hr OCP at the end in 0.6M NaCl, 25C.*

From the galvanostatic treatments, a combination of the applied current and time of exposure allows the OCP to reach the low cracking regime. There appears to be a maximum level of ennoblement as reflected in the post-dissolution OCP of around -600 mV$_{SCE}$ for this particular ZnNi plating composition and thickness. From the cyclic exposures conducted at 1mA cm^{-2}, it can be seen that dissolution past the upper limit to the ennoblement there is a decrease in the OCP. Looking at the surface post Zn dissolution, SEM micrographs reveal that the surface morphology is entirely different, Figure 9. The OCP measured on the surface after exposure was -0.605V$_{SCE}$ which is within the immunity well. After exposure, it appears as though the ZnNi coating has been almost entirely removed as there is no longer any resemblance to the microstructure prior to exposure.

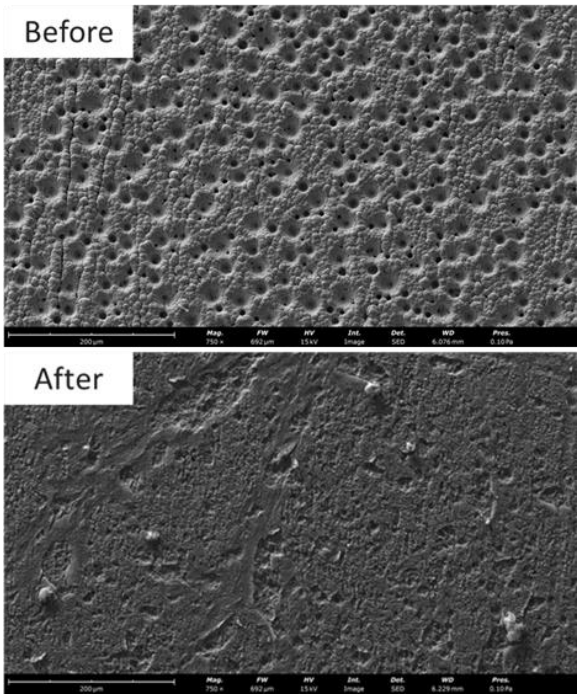

Figure 9. *SEM micrographs of the ZnNi plating surface (plan view) from before and after galvanostatic treatments (exposure 10mA cm^{-2} for 60 min in 0.6M NaCl).*

This loss of coating was also confirmed with EDS that showed strong Fe peaks and other elemental peaks from the substrate material with little Zn and Ni remaining. Figure 10 shows a micrograph taken on a cross sectioned sample near the outside line of exposure to include the bulk exposed surface area and the area underneath the o-ring. This particular sample has reached the immunity well with OCP measured at -0.692V$_{SCE}$ after the galvanostatic treatment.

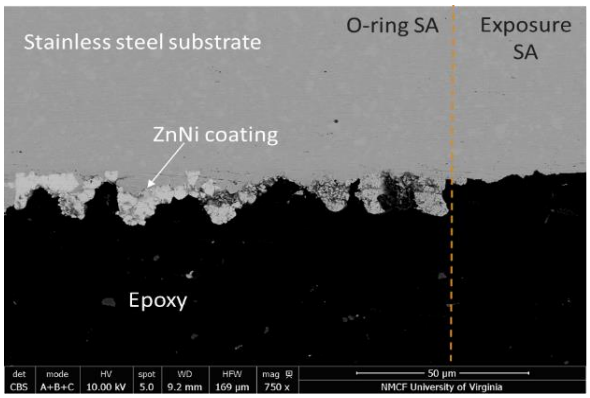

Figure 10. *SEM micrograph of the ZnNi plating surface (cross section) after galvanostatic treatment (exposure at 1mA cm^{-2} for 9 hours) and ammonium acetate cleaning (1.3M, 70°C, 5 min).*

The SEM micrograph of the cross section further corroborated that all or nearly all of the ZnNi plating in the bulk surface area exposed has been removed through the galvanostatic treatment in order to reach the ennoblement into the immunity well.

FEM Modeling Results

Paired with the electrochemical measurements in the laboratory, FEM modelling was used to understand the impacts of material combinations, geometry, and different wetting circumstances that may occur. Using experimentally determined boundary conditions, the FEM model is able to simulate and predict the potential distribution over the multi-component fastener plate assembly given material kinetics in a given electrolyte.

A series of analyses were conducted looking at variability in the P675 kinetics, impact of ZnNi and P675 surface areas, partial wetting scenarios, and changing ZnNi kinetics. Figure 11 shows the spread of variability in the P675 anodic kinetics as well as the impact that has on the potential predicted down the fastener hole. These predictions of the potential down hole were made using two different material combinations: all anodic material as the P675 and with a ZnNi plating applied to the top surface of component 1. In all instance of plotting the potential down the hole, the zero mark is for the top of the hole, at the surface of the first component. The large amount of variability in the P675 kinetics and the simulations conducted to see their impact helps to rationalize why there is not always cracking occurring in service. Based on the kinetics of the P675, there will be higher or lower risk of cracking as the potential down the fastener hole may in fact be in the low cracking regime as seen in Figure 11. The incorporation of ZnNi did not have a significant impact in this scenario, likely due to the large amount of P675 area.

Further simulations with less WL penetration down the fastener hole were also conducted. Figure 12 shows the geometry used in the simulations as well as the potential profile down the fastener hole for the varying WL ingress.

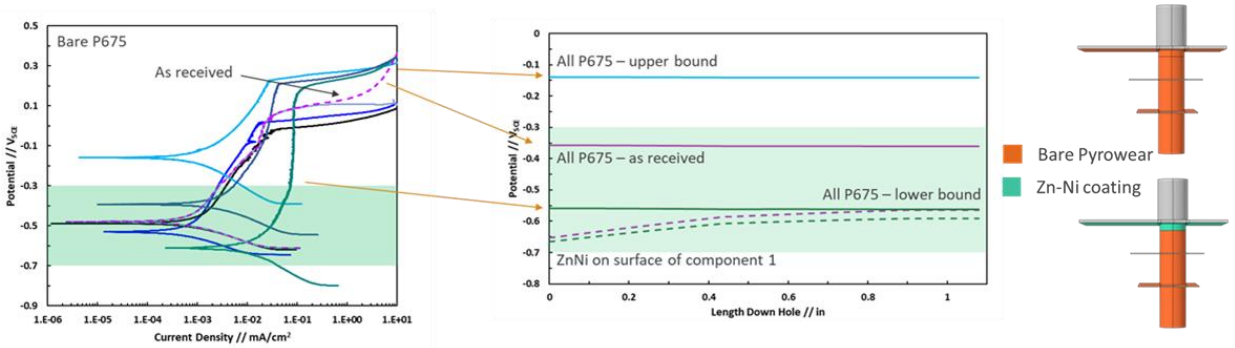

Figure 11. *Anodic PDS curves in 0.6M NaCl collected on bare P675 (400 grit SiC) and as-received state as well as the predicted potential down the fastener hole for three kinetic options (highest anodic bound, lowest, and as received surface) and what happens with the addition of ZnNi on the surface; the multi-material combinations for the two scenarios used in these modelling predictions.*

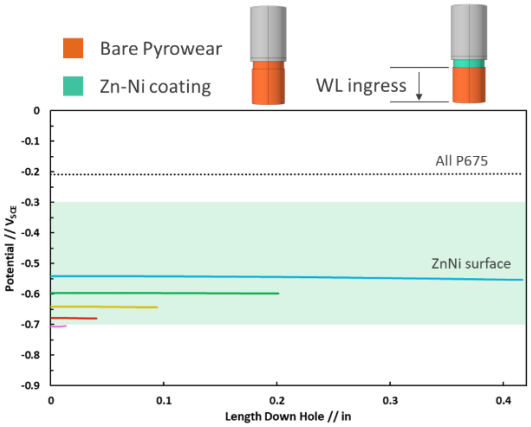

Figure 12. *Geometry built for the WL ingress study as well as the corresponding potential profiles down hole for the varying degrees of wetness.*

In this string of models, the WL was built to be 1, ½, ¼, 1/8, 1/16 of length of the component 1 bore hole. ZnNi coating was applied on the surface only underneath the fastener head. As the amount of wetted P675 is decreased, the potential down the fastener hole is slowly decreasing due to the ability of the ZnNi plating to polarize the assembly down towards its OCP. Due to the ratio of the WL in contact with the anodized Ti included in this set of simulations, the ZnNi is not able to fully polarize the P675 all the way down to its OCP. In situations with very little WL down the fastener hole, there becomes a risk of over polarization. That risk will increase if the WL conformal over the anodized Ti fastener head diminishes or dries up entirely, removing the counterbalance of the ZnNi.

Considering other wetting scenarios, the WL may not be on the surface but rather only down the fastener hole in the instance where the surface dries first in service and the occluded crevices in the assembly will take longer to dry out. Additionally, there could be states of partial wetting down hole without surface wetting.

Taking a deeper dive into the partial wetting and using those scenarios to understand the impact of changing ZnNi kinetics over time is important. To that end, the kinetics of ZnNi from an initial state (30 min) up to 10 weeks have been used as boundary conditions for the modeling. The predicted potential profile down the fastener hole can be seen in Figure 13.

Up until the 6-week time point, the ZnNi kinetics indicate that there would be a risk of cracking if the coating were applied without any alteration or post processing to enrich the surface with Ni. The top 30% of the hole would be at risk of cracking in a full wetting scenario down hole without surface wetting. In the case where there is partial wetting down hole, the ZnNi is able to polarize the P675 down all the way to its OCP.

Discussion

Controlling the Ni content is critical is devising a fail-safe solution to the SCC using Zn-Ni

From the galvanic exposure of ZnNi-P675 couples conducted with the 1:1 area ratio, there was an inclination that the Zn-15.8%Ni may be too polarizing at it is with the normal plating bath and composition from Techmetals. The ZnNi plating has highly active anodic kinetics, which allows for it to be able to pull the P675 all the way or nearly all the way down to its OCP even with a small

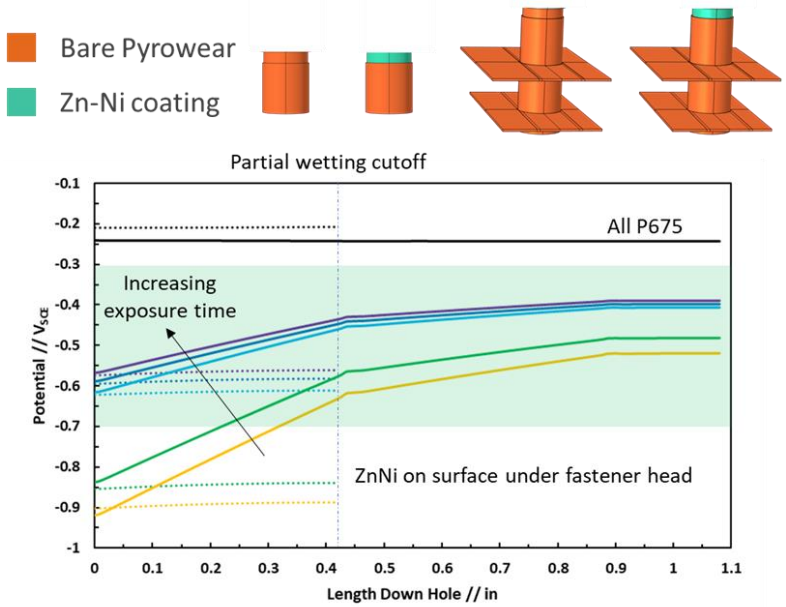

Figure 13. *Potential profile down the fastener hole for 30 min, 3 week, 6 week, 9 week, and 10 week ZnNi kinetics for ZnNi plating applied on the surface under the fastener head only for both full wetting down hole and partial wetting down hole.*

surface area. This extent of polarization was observed through the simulations conducted with reduced WL ingress down the fastener hole without WL extending over the anodized Ti fastener head. As the kinetics of the ZnNi change with increasing time of exposure, the OCP increases. This effect is attributed to the selective removal of the Zn from the bi-metallic matrix and simultaneous enrichment of the Ni. Through the Zn dissolution, the Ni was observed to rise upwards of 25 wt.%, which contributed to the observation of the ennobling of the OCP for the ZnNi plating. This ennoblement will occur naturally with exposure at OCP, albeit slowly. Thus, forced galvanostatic dissolution of Zn was employed to speed up the enrichment process. In this manner, with a range of currents and times, the ZnNi OCP was ennobled to reach the low cracking regime in 0.6M NaCl successfully (Figure 8). It was found that the lower current (1 mA cm^{-2}) was the most reproducible for ensuring ennoblement of the ZnNi OCP up to the immunity well for both cyclic and continuous galvanostatic exposures. Between the cyclic and continuous galvanostatic treatments, the cyclic exposures provided a higher ceiling for ennoblement with a more stable OCP after treatment.

Leveraging the enrichment of Ni is critical in preventing the over polarization of the P675 from the ZnNi plating to provide a solution to the SCC problem that does not run the risk of increasing the cracking by polarizing to the other side of the immunity well (<-700 mV_{SCE}).

It is feasible to create a condition in which the implementation of ZnNi coating could lead to a fail-safe polarization precluding over polarization of the P675 by the ZnNi into the low potential cracking regime. The fail-safe condition occurs if a ZnNi coating with a sufficiently high OCP can be obtained either by control of the initial plating composition or via post-processing via selected dissolution of Zn. The ZnNi plating cannot polarize the P675 more negative than the OCP of the ZnNi. Thus, if the ZnNi OCP is in the safe regime of potential, the use of ZnNi would allow protection from cracking.

Modeling the most relevant WL scenarios indicated risk of cracking from over polarization

In all circumstances with just P675 and anodized Ti, the model predicted that there would be cracking if the most frequent anodic and cathodic kinetics for P675 were used as boundary conditions. Assuming a full wetting scenario where the electrolyte penetrates to all surfaces on the multi-component assembly indicates that nearly any application of the ZnNi plating will resolve the cracking problem. The potential down the hole being in the immunity well in all of the initial plating scenarios with full wetness is attributed to the large amount of P675 and the large tolerances in the assembly that allows for the polarization of the ZnNi to be distributed over the whole assembly. This result is unlikely to occur in service as there will likely be less surface wetting and potentially less WL penetration down the fastener hole.

Modeling predictions with reduced wetting indicated that there would be situations where the ZnNi would over polarize the P675 substrate past the bottom of the immunity well and allow for cracking to occur. Reducing the amount of ZnNi present on the assembly greatly reduced that risk. If the ZnNi was only applied underneath the fastener head, there were many less scenarios that indicated a risk of cracking with the initial kinetics of the standard ZnNi plating (15.8 wt.% Ni as determined by the manufacturers). The incorporation of ZnNi kinetics from different exposure times into the partial wetting models demonstrated that for the initial and even 3-week kinetics that crack formation can be expected due to the polarizability of the ZnNi (Figure 13). Once the ZnNi has be enriched in Ni enough, this was no longer an expected risk.

Conclusions

Electrochemical measurements

- There is significant variability in the ZnNi OCP from different batches of plating from TM (200mV).
- The ZnNi plating is highly polarizing, taking the P675 down to OCP of ZnNi upon galvanic coupling at a 1:1 area ratio.
- ZnNi plating undergoes slow ennoblement in an isolated exposure, increasing kinetics observed up to 10 weeks, ultimately reaching the low cracking regime in 0.6M NaCl.
- The ennoblement observed on the ZnNi plating is attributed to enrichment of the Ni with dissolution of Zn.
- Lower current density and cyclic exposure appear to be most helpful in more consistently reaching the immunity well in 0.6M NaCl.

- OCP of ZnNi after the forced dissolution is stable.

Modeling

- The large variability in the P675 kinetics cause complications in vast swings of OCP predicted, making it hard to know the electrochemical behavior of the materials when they are in service. This result also provides a rationalization for the random occurrences of cracking in service.
- Surface wetting with reduced down hole solution penetration can cause over polarization with ZnNi plating application.
- ZnNi has large capacity to polarize and bring P675 down to its OCP even with small surface areas. This leads to the need for a fail-safe ZnNi that has an OCP in immunity well to remove the risk of over polarization.
- Ennoblement of OCP for ZnNi plating greatly reduces the cracking risk.

Acknowledgements

Funding both from the Virginia Space Grant Consortium fellowship program and the Olsen Fellowship at the University of Virginia is greatly appreciated. The financial and technical support from J. Cook, A. Heeter, B. Wiley, B. Drier, C. Schumacher, and S. Conn from the Rolls-Royce Corporation was influential in the completion of this work. Collaborations with the Burns research group at the University of Virginia was greatly appreciated. Any opinions, conclusions, and recommendations stated here are those of the author(s).

References

(1) Marshall, R. S.; Harris, Z. D.; Small, M. K.; Brunner, K. L.; Burns, J. T.; Kelly, R. G. A Materials Selection Framework for Fastener-in-Panel Geometries Using FEM and LEFM, to Mitigate Coating Degradation and Environmentally Assisted Cracking. *Corros. Sci.* **2024**, *227* (August 2023), 111788. https://doi.org/10.1016/j.corsci.2023.111788.

(2) Harris, Z. D.; Marshall, R. S.; Kelly, R. G.; Burns, J. T. Coupling Fracture Mechanics Experiments and Electrochemical Modeling to Mitigate Environment-Assisted Cracking in Engineering Components. *Corrosion* **2023**, *79* (3), 363–375. https://doi.org/10.5006/4244.

(3) Gangloff, R. P. Hydrogen Assisted Cracking of High Strength Alloys. *Compr. Struct. Integr.* **2003**, *6*, 31–101.

(4) Steiner, P. J.; Harris, Z. D.; Vicente Moraes, C.; Kelly, R. G.; Burns, J. T. Investigation of IG-SCC Growth Kinetics in Al-Mg Alloys in Thin Film Environments. *Corrosion* **2021**, *77* (8), 838–852. https://doi.org/10.5006/3833.

(5) Galvele, J. R. 1999 W.R. Whitney Award Lecture: Past, Present, and Future of Stress Corrosion Cracking. *Corrosion* **1999**, *55* (8), 723–731. https://doi.org/10.5006/1.3284027.

(6) Charles-Granville, U.-E.; Marshall, R. S.; Moraes, C. V.; Glover, C. F.; Scully, J. R.; Kelly, R. G. Application of Finite Element Modeling to Macro-Galvanic Coupling of AA7050 and SS316: Validation Using the Scanning Vibrating Electrode Technique. *J. Electrochem. Soc.* **2022**, *169* (3), 031502. https://doi.org/10.1149/1945-7111/ac55ce.

(7) Cocke, C.; Marshall, R. S.; Sprinkle, C.; Goff, A.; Kelly, R. G.; Burns, J. T. The Effect of Corrosion Location Relative to Local Stresses on the Fatigue Life of Geometrically Complex, Galvanically Corroded AA7075-T6. *Corrosion* **2022**, *78* (2), 152–162. https://doi.org/10.5006/3908.

(8) Lee, Y.; Gangloff, R. P. Measurement and Modeling of Hydrogen Environment-Assisted Cracking of Ultra-High-Strength Steel. *Metall. Mater. Trans. A Phys. Metall. Mater. Sci.* **2007**, *38 A* (13), 2174–2190. https://doi.org/10.1007/s11661-006-9051-z.